Conference Paper, Published Version

Bollaert, Erik F. R.; Vrchoticky, B.; Falvey, H. T.

Extreme Scour Prediction at High-Head Concrete Dam and Stilling Basin (United States)

Extreme Scour Prediction at High-Head Concrete Dam and Stilling Basin (United States)

E.F.R. Bollaert*, B. Vrchoticky ** and H.T. Falvey***
* AquaVision Engineering Ltd., Lausanne, Switzerland
** US Army Corps of Engineers, United States
*** H.T. Falvey & Associates, Colorado, United States

I. INTRODUCTION

This paper presents the application of a recently developed physics based model that predicts scour formation downstream of large dam spillways (Bollaert, 2004). The model is based on experiments with air-water jets impinging on jointed media and related numerical modeling of involved physical phenomena. It predicts the ultimate scour depth and the time development of scour formation in different types of fissured media. The model is under continuous development and has been applied to several scour cases worldwide. The model includes several physics based modules for scour prediction that are based on the resistance of the medium to fissure initiation and propagation, as well as on the resistance of individual blocks to sudden ejection.

A case study of a High-Head Concrete Dam and Stilling Basin as shown in figure 1, located in the United States, is presented here. The dam in question has experienced several large storm events during the last twenty years, with maximum spillway releases of up to about 4,000 m^3/s. The latest hydrology developed in lieu of these events indicates that for the Probable Maximum Flood (PMF), releases from the dam could exceed 22,700 m^3/s, while the original design PMF was only 15,600 m^3/s.

Hence, modifications to the outlet works are being studied to increase the flood discharge capacity by increasing the gate size and adding two additional gates. The larger jets issuing from the modified outlet works impact against a stilling basin that was originally designed mainly as a hydraulic jump energy dissipater. There is no true plunge pool for the jets and tailwater is relatively shallow.

The present paper describes detailed numerical computations made to predict the ultimate possible scour depth in the rock formation downstream of the dam following a failure of the concrete lining of the stilling basin. The computations have been made for both the emergency design flood through the 3 emergency spillway gates (8,500 m^3/s) and for the new PMF event (22,700 m^3/s). A 3D assessment of scour hole formation and its time development in the rock mass downstream of the dam has been obtained. The computations indicate that, during the design flood, scour will remain quite local, while for the PMF event, failure of the concrete lining might result in severe scour formation of the rocky foundation just downstream of the dam.

a) General view of dam and stilling basin

b) Downstream view of stilling basin and channel

Figure 1.

II. MAIN CHARACTERISTICS OF DAM AND STILLING BASIN

The geometry of the dam and downstream stilling basin is shown in Figure 2. The dam is a concrete gravity dam equipped with 5 service spillway gates and 3 emergency spillway gates. In addition to these gates, the dam also incorporates 10 intermediate outlet works, with dimensions of 3m by 4m (4 lower tiers) and 3m by 4.5 m (6 upper tiers) The dam is able to pass excess water from the reservoir in two different ways: by means of crest overflows along the downstream face (chute) of the dam and by means of a series of pressurized outlets (jet flow) through the dam body. The jets from the outlets impact the downstream stilling basin.

The stilling basin floor consists of concrete slabs and sidewalls and measures about 75 m wide by 110 m long. The upstream boundary is formed by a smooth curve at the dam toe, while the downstream boundary is formed by an end sill. The concrete slabs have a thickness of about 1.5 m, with horizontal dimensions of 15m by 15m (square slabs) or 6m by 15m (rectangular slabs).

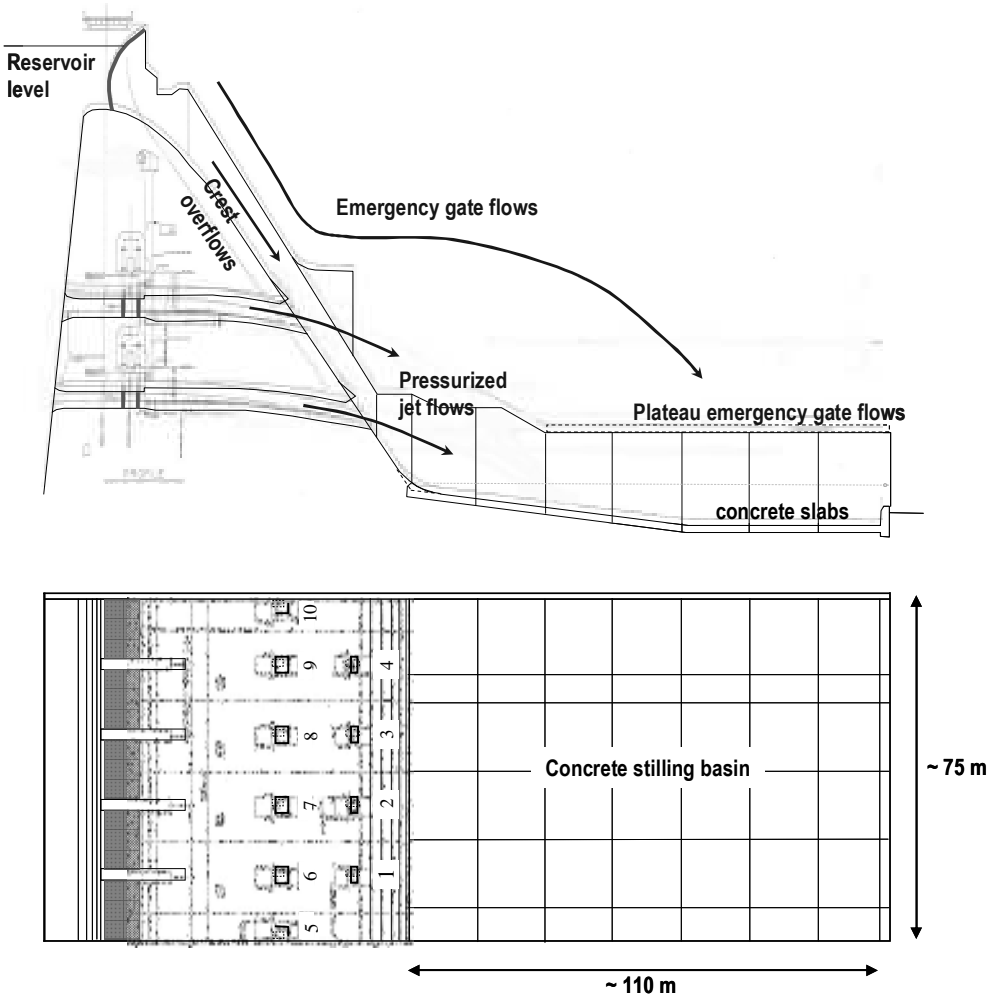

Figure 2. Plan view and cross-sectional view of high-head dam and stilling basin

III. ROCK MASS CHARACTERISTICS

The rock mass at the dam site is described as a hard and durable Sierra granite/quartz diorite, medium to coarse grained, with an Unconfined Compressive Strength (UCS) of about 130 MPa. Based on drainage gallery core drilling, the RQD (Rock Quality Designation) has been estimated at 75-90 %. The rock is slightly to moderately weathered and is generally considered to provide a good erosion resistant surface. Nevertheless, one of the most serious problems encountered during dam construction was the depth of weathering. This depth depends on the average joint spacing and on micro fracturing of the grains. Most weathering was found to start by alteration along the joints, due to water flowing through these planes. Moreover, the rock is intersected by faults, shear zones and different main joint sets. Zones of sheared rock of up to more than 1m thick are also present. These zones are nearly vertical, but most probably do not interfere with the stilling basin rocky foundation.

IV. Comprehensive Scour Model (Bollaert, 2004)

A new and physics based scour prediction model was developed at the Laboratory of Hydraulic Constructions of the Swiss Federal Institute of Technology in Lausanne, Switzerland (Bollaert, 2002 and 2004; Bollaert & Schleiss, 2005). The model uses physical laws and phenomena that have been simplified to allow its application to practical engineering projects. It is based on experimental and numerical investigations of dynamic water pressures in rock joints (Bollaert, 2002).

The model comprises two methods that describe failure of fractured rock. The first one, the Comprehensive Fracture Mechanics (CFM) method, determines the ultimate scour depth by expressing instantaneous or time-dependent joint propagation due to water pressures jacking inside the joint. The second one, the Dynamic Impulsion (DI) method, describes the ejection of rock blocks from their mass due to sudden uplift pressures.

The structure of the Comprehensive Scour Model consists of three modules: the falling jet, the plunge pool and the rock mass. The latter module implements the two aforementioned failure criteria. More details can be found in Bollaert (2004) or Bollaert & Schleiss (2005).

A. *Falling jet Module*

This module describes how the hydraulic and geometric characteristics of the jet are transformed from the free falling jet down to the plunge pool as shown in Figure 3. Three parameters characterize the falling jet: the velocity V_i, the diameter (or width) D_i and the initial turbulence intensity Tu, defined as the ratio of velocity fluctuations to the mean velocity.

The jet trajectory is based on ballistics and air drag and will not be further outlined. The jet module computes the longitudinal location of impact, the total trajectory length L and the velocity and diameter at impact V_j and D_j. The turbulence intensity is presented in the next paragraph and defines the spread of the jet δ_{out} (Ervine et al., 1997). Superposition of the outer spread to the initial jet diameter D_i results in the outer jet diameter D_{out}, which is used to determine the extent of the zone at the water-rock interface where severe pressure damage may occur. The relevant relationships are:

$$Tu = u'/U \tag{1}$$

$$\frac{\delta_{out}}{X} = 0.38 \cdot Tu \tag{2}$$

$$D_j = D_i \cdot \sqrt{\frac{V_i}{V_j}} \tag{3}$$

$$V_j = \sqrt{V_i^2 + 2gZ} \tag{4}$$

$$D_{out} = D_i + 2 \cdot \delta_{out} \cdot L \tag{5}$$

in which δ_{out} is the half angle of outer spread, X the longitudinal distance from the point of issuance and Z the vertical fall distance of the jet. Typical outer angles of jet spread are 3-4 % for roughly turbulent jets (Ervine & Falvey, 1987). The corresponding inner angles of jet spread are 0.5 - 1 %.

The angle of the jet at impact is neglected, which is reasonable for impingement angles that are close to the vertical (70-90°). For smaller impingement angles, the water depth Y is defined as the exact trajectory length of the jet through the water cushion, and not as the vertical difference between water level and pool bottom.

B. *Plunge Pool Module*

This module describes the hydraulic and geometric characteristics of the jet when traversing the plunge pool and defines the water pressures at the water-rock interface. The plunge pool water depth Y is essential. For near-vertically impacting jets, it is defined as the difference between the water level and the bedrock level at the point of impact. The water depth increases with discharge and scour formation. Initially, Y equals the tailwater depth t as shown in Figure 4. During scour formation, Y has to be increased with the depth of the formed scour h. Prototype observations indicate possible mounding at the downstream end of the pool. This mounding results from detached rock blocks that are swept away and that deposit immediately downstream. This can raise the tailwater level. The effect is not directly described in the module but can easily be added to the computations by appropriate modification of the water depth during scour.

The water depth Y and jet diameter at impact D_j determine the ratio of water depth to jet diameter at impact Y/D_j. This ratio is directly related to jet diffusion. Precaution should be taken when applying this parameter. Significant differences may exist in practice due to the appearance of vortices or other surface disturbing effects, which can change the effective water depth in the pool. Again, engineering judgment is required on a case-by-case basis.

Dynamic pressures acting at the water-rock interface are generated by core jet impact for small water depths Y, or by developed jet impact (shear layer), for Y/D_j greater than 4 to 6 (for plunging jets) as shown in Figure 4. The most relevant pressure characteristics are the mean dynamic pressure coefficient C_{pa} and the root-mean-square (rms) coefficient of the fluctuating dynamic pressures C'_{pa}, both measured directly under the centerline of the jet. These coefficients correspond to the ratio of pressure head (in [m]) to incoming kinetic energy of the jet ($V^2/2g$) and are defined as follows:

$$C'_{pa} = 0.00022 \cdot \left(\frac{Y}{D_j}\right)^3 + 0.0079 \cdot \left(\frac{Y}{D_j}\right)^2 + 0.0716 \cdot \left(\frac{Y}{D_j}\right) + \eta \tag{6}$$

$$C_{pa} = 38.4 \cdot (1 - \alpha_i) \cdot \left(\frac{D_j}{Y}\right)^2 \quad \text{for } Y/D_j > 4\text{-}6 \tag{7}$$

$$C_{pa} = 0.85 \qquad \text{for } Y/D_j < 4\text{-}6 \tag{8}$$

$$\alpha_i = \frac{\beta}{1+\beta} \tag{9}$$

Equations 7 through 9 are based on Ervine et al. (1997). The air concentration at jet impact α_i is defined as a function of the volumetric air-to-water ratio β. Plausible prototype values for β are 1-2. For a given α_i, mean and fluctuating dynamic pressures are defined as a function of Y, D_j and Tu. Similar expressions are proposed at locations radially outwards from the jet's centerline and can be found in Bollaert (2002). Tu is assumed representative for low-frequency fluctuations, which define the stability of the jet during its fall. Hence, Tu can be related to the root-mean-square (rms) values of the pressure fluctuations at the pool bottom. This is essential because these fluctuations generate peak pressures inside underlying rock joints.

From equation 6, the rms values of the pressure fluctuations at the pool bottom (C'_{pa}) depend on Y/D_j and Tu. The parameter η of equation 6 represents the degree of jet stability: η is equal to 0 for compact jets and goes up to 0.15 for highly turbulent and unstable jets. Compact jets

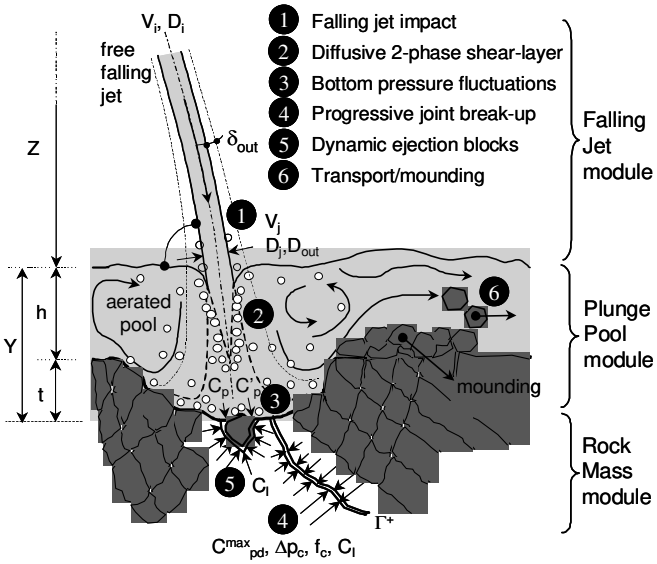

Figure 3. Main parameters of scour and its physical phenomena (Bollaert, 2004)

(Tu < 1%) are smooth during their fall, without any instability. Highly turbulent jets have a Tu > 5%. In between, for 1% < Tu < 5%, η has to be chosen between 0 and 0.15 as a function of jet stability effects.

Generally, Tu is unknown. Under such circumstances, estimation can be made based on the type of outlet structure (Bollaert et al., 2002). For example, a free overfall jet has an estimated Tu of 1-3 %, a ski jump 3-5 %, and intermediate or bottom outlets 5-8 %. However, Tu may largely depend on the outlet geometry, the flow pattern upstream, etc. These aspects should be accounted for by appropriate engineering judgment.

C. Rock Mass Module

The pressures defined at the bottom of the pool are used for determination of the transient pressures inside open-end or closed-end rock joints. The parameters are:

1. maximum dynamic pressure coefficient C^{max}_p
2. characteristic amplitude of pressure cycles Δp_c
3. characteristic frequency of pressure cycles f_c
4. maximum dynamic impulsion coefficient C^{max}_I

The first parameter is relevant to brittle propagation of closed-end rock joints. The second and third parameters express time-dependent propagation of closed-end rock joints. The fourth parameter is used to define dynamic uplift of rock blocks formed by open-end rock joints. The maximum dynamic pressure C^{max}_p is obtained through multiplication of the rms pressure C'_{pa} with an amplification factor Γ^+, and by superposition with the mean dynamic pressure C_{pa}. Γ^+ expresses the ratio of the peak value inside the rock joint to the rms value of pressures at the pool bottom and has been determined based on prototype-scaled experiments (Bollaert, 2004).

The product of C'_{pa} times Γ^+ results in a maximum pressure, written as (Bollaert, 2002):

$$P_{\max}[Pa] = \gamma \cdot C_p^{\max} \cdot \frac{V_j^2}{2g} = \gamma \cdot \left(C_{pa} + \Gamma^+ \cdot C'_{pa}\right) \cdot \frac{V_j^2}{2g} \tag{10}$$

The main uncertainty of equation 10 lies in the Γ^+ factor. The characteristic amplitude of the pressure cycles, Δp_c, is determined by the maximum and minimum

pressures of the cycles. The characteristic frequency of pressure cycles f_c follows the assumption of a perfect resonator system and depends on the air concentration in the joint α_i and on the length of the joint L_f.

Beside the dynamic pressure inside rock joints, the resistance of the rock also has to be determined. The cyclical character of the pressures generated by the impact of a high-velocity jet makes it possible to describe joint propagation by *fatigue* stresses occurring at the tip of the joint. This can be described by Linear Elastic Fracture Mechanics (LEFM).

A simplified methodology is used (Bollaert, 2004). It is called the *Comprehensive Fracture Mechanics (CFM) method* and applicable to any type of partially jointed rock. Pure tensile pressure loading inside rock joints is described by a stress intensity factor K_I, which represents the amplitude of the stresses that are generated by the water pressures at the tip of the joint. The corresponding resistance of the rock mass to joint propagation is expressed by its fracture toughness K_{Ic}.

Joint propagation distinguishes between brittle (or instantaneous) joint propagation and time-dependent joint propagation. The former happens for a stress intensity factor that is equal to or higher than the fracture toughness of the material. The latter is occurring when the maximum possible water pressure results in a stress intensity that is inferior to the material's resistance. Joints may then be propagated by fatigue. Failure by fatigue depends on the frequency and the amplitude of the load cycles. The fracture mechanics implementation of the hydrodynamic loading consists of a transformation of the water pressures in the joints into stresses in the rock. These stresses are characterized by K_I as follows:

$$K_I = P_{\max} \cdot F \cdot \sqrt{\pi \cdot L_f} \qquad (11)$$

in which K_I is in MPa$\sqrt{}$m and P_{max} in MPa. The boundary correction factor F depends on the type of crack and on its persistency, i.e. its degree of cracking defined as a/B or b/W in Figure 5. This figure presents two basic configurations for partially jointed rock. The choice of the most relevant geometry depends on the type and the degree of jointing of the rock.

The first crack is of semi-elliptical shape and partially sustained by the surrounding rock mass in two horizontal directions. Corresponding stress intensity factors should be used in case of low to moderately jointed rock. The second crack is single-edge notched and of two-dimensional nature. Support from the surrounding rock mass is only exerted perpendicular to the plane of the notch and, as a result, stress intensity factors will be substantially higher. Thus, it is appropriate for significantly to highly jointed rock.

In practice, F values of 0.5 or higher are considered to correspond to completely broken-up rock, i.e. the DI method becomes more applicable than the CFM method. For values of 0.1 or less, a tensile strength approach is more plausible. However, most of the values in practice can be considered between 0.20 and 0.40, depending on the type and number of joint sets, the degree of weathering, distances between joints, etc.

The fracture toughness K_{Ic} has been related to the mineralogical type of rock and to the unconfined compressive strength UCS. Furthermore, corrections are made to account for the loading rate and the in-situ stress field. The corrected fracture toughness is defined as the in-situ fracture toughness $K_{I,\ ins}$ and is based on a linear regression of available literature data.

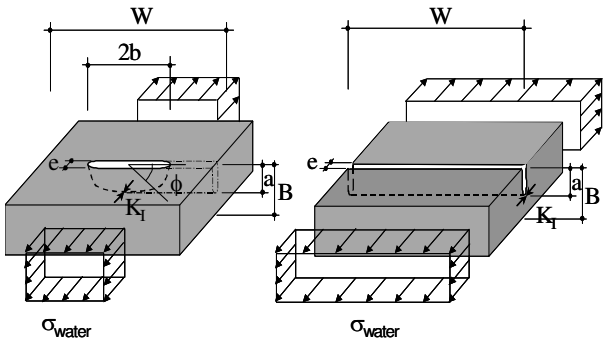

Figure 4. Rock joint parameters (Bollaert, 2004)

$$K_{I\ ins,\ UCS} = (0.008\text{-}0.010)\cdot UCS + (0.054\cdot\sigma_c) + 0.42 \qquad (12)$$

in which σ_c represents the confinement horizontal in-situ stress and T, UCS and σ_c are in MPa. Instantaneous joint propagation will occur if $K_I \geq K_{I,ins}$. If this is not the case, joint propagation is expressed by an equation as originally proposed to describe fatigue growth in metals:

$$\frac{dL_f}{dN} = C_r \cdot \left(\Delta K_I / K_{Ic}\right)^{m_r} \qquad (13)$$

in which N is the number of pressure cycles. C_r and m_r are material parameters that are determined by fatigue tests and ΔK_I is the difference of maximum and minimum stress intensity factors. To implement time-dependent joint propagation into the model, m_r and C_r have to be known. They represent the vulnerability of rock to fatigue and can be derived from available literature data on quasi-steady break-up by water pressures in joints (Atkinson, 1987). A calibration for granite (Cahora-Bassa Dam; Bollaert, 2002) resulted in C_r = 1E-8 for m_r = 10.

The fourth dynamic parameter is the maximum dynamic impulsion $C^{max}{}_I$ in an open-end rock joint (underneath single block), obtained by time integration of net forces on the block:

$$I = \int_0^{\Delta tpulse} \left(F_u - F_o - G_b - F_{sh}\right)\cdot dt = m \cdot V_{\Delta tpulse} \qquad (14)$$

in which F_u and F_o are the forces under and over the block, G_b is the submerged weight of the block and F_{sh} represents the shear and interlocking forces. The shape of a block and the type of rock define the immerged weight. Shear and interlocking forces depend on the joint pattern and the in-situ stresses. As a first approach, they can be neglected. The pressure field over the block is governed by jet diffusion. The pressure field under the block corresponds to transient pressure waves. The first step is to define the maximum net impulsion I^{max}. I^{max} is defined as the product

of a net force and a time period. The corresponding pressure is made non-dimensional by the jet's kinetic energy $V^2/2g$. This results in a net uplift pressure coefficient C_{up}. The time period is made non-dimensional by the travel period that is characteristic for pressure waves inside rock joints, i.e. $T = 2 \cdot L_j/c$. This results in a time coefficient T_{up}. Hence, the non-dimensional impulsion coefficient C_I is defined by the product $C_{up} \cdot T_{up} = V^2 \cdot L/g \cdot c$ [m·s]. The maximum net impulsion I^{max} is obtained by multiplication of C_I by $V^2 \cdot L/g \cdot c$. Prototype-scaled analysis of uplift pressures resulted in the following expression for C_I:

$$C_I = 0.0035 \cdot \left(\frac{Y}{D_j}\right)^2 - 0.119 \cdot \left(\frac{Y}{D_j}\right) + 1.22 \qquad (15)$$

Failure of a block is expressed by the displacement it undergoes due to the net impulsion coefficient C_I. This is obtained by transformation of $V_{\Delta tpulse}$ in equation 14 into a net uplift displacement h_{up}. The net uplift displacement that is necessary to eject a rock block from its matrix is difficult to define. It depends on the protrusion and the degree of interlocking of the blocks. A calibration on Cahora-Bassa Dam (Bollaert, 2002) resulted in a critical net uplift displacement of 0.20.

V. APPLICATION OF CSM MODEL

The Comprehensive Scour Model has been applied to the stilling basin of this case study. The model has applied parametric values as presented in Table 1 to estimate scour formation in the rocky foundation following failure of the concrete slabs of the stilling basin. The time development of scour has been defined at time intervals of 1h, 6h, 12h, 24h, 4 days, 8 days, 100 and finally 200 days of discharge.

TABLE I. MAIN GEOMECHANICAL PARAMETERS USED BY THE CSM MODEL

	Parameter	Symbol	Unit	VALUE
Fracture Mechanics	Type of rock	-	-	granite
	Unconfined Compressive Strength	UCS	MPa	131
	In-situ stress ratio	K_0	-	0
	Joint wave celerity for break-up	c	m/s	150
	Amplification factor G	-	-	2
	Number of joint sets	N_j	-	3
	Typical maximum joint length	L	m	1
	Initial break-up of joint	P	-	varies
	Form of joints	-	-	varies
	Fatigue sensibility	m_f	-	10
	Fatigue coefficient	C_f	-	1.00E-07
Dynamic Impulsion	Ratio height/side length of block	h_b/l_b	-	0.25
	Density rock	γ_r	kg/m^3	2650
	Joint wave celerity for uplift	c	m/s	100

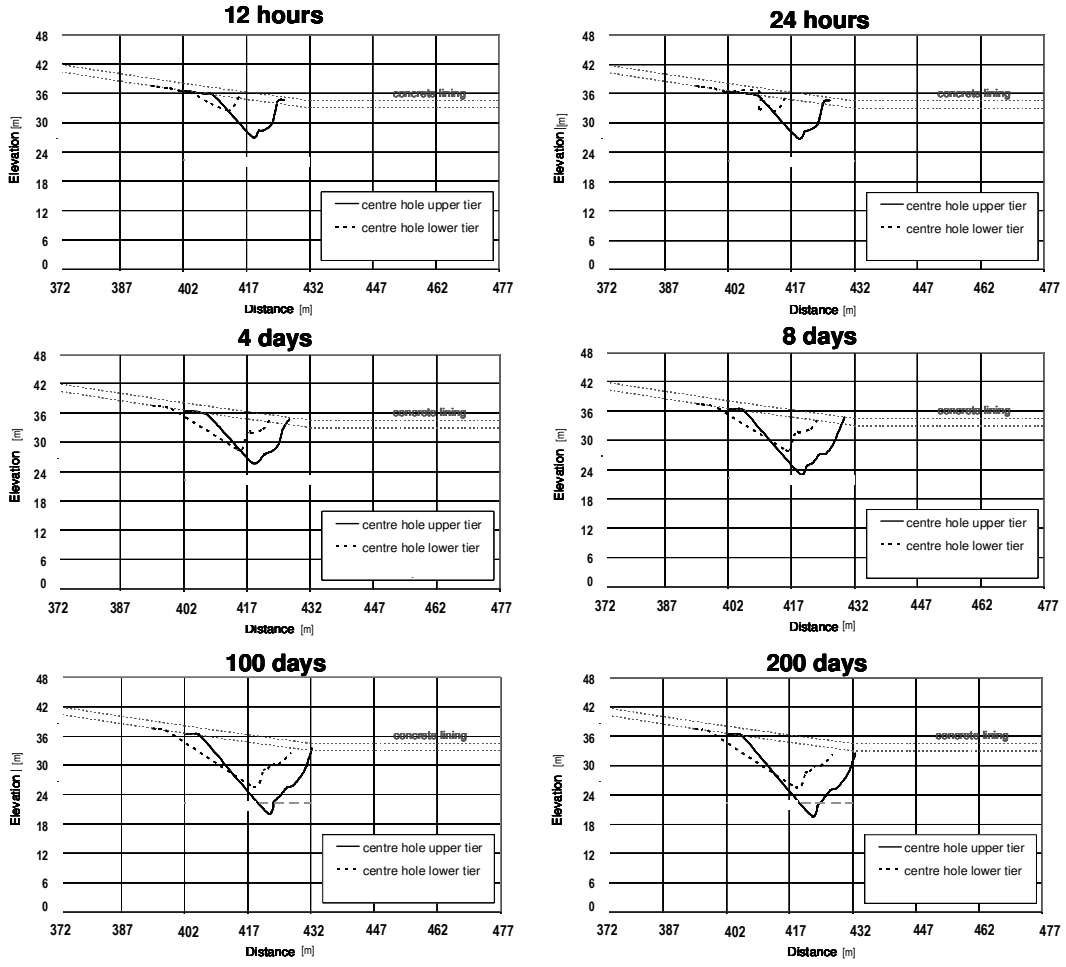

Figure 5. Scour formation as a function of time in stilling basin for a constant discharge of 3,300 cms and following the parametric assumptions of Table 1 (Comprehensive Fracture Mechanics Model, Bollaert 2004).

A. Scour formation for flood event of 3,300 cms

First, potential scour formation in the stilling basin and following failure of the concrete slabs has been estimated for a regular flood event that is transferred towards downstream via the pressurized outlet works. The flood discharge is assumed constant and defined at 3,300 cms.

Figure 5 presents scour formation as a function of the time duration of the flood event. Each of the figures represents a longitudinal section of the stilling basin, showing the initial elevation of the concrete slabs and the depth and the general shape of the formed scour hole. Based on the Comprehensive Fracture Mechanics Model, it can be seen that scour rapidly forms during the first few days and that subsequent scour takes much more time to happen. After 200 days of constant discharge, the scour hole has attained a maximum depth of 15 m. Figure 6 presents the corresponding three-dimensional perspective view, showing the shape of the scour holes formed in the rock mass underneath the stilling basin. The part of the stilling basin that is represented on this figure corresponds to the sloped (upstream) part, with a total length of about 60 m. When applying the Dynamic Impulsion Model, the ultimate scour depth for the same constant discharge is situated at 15.5 m, i.e. very close to the former results after 200 days of discharge.

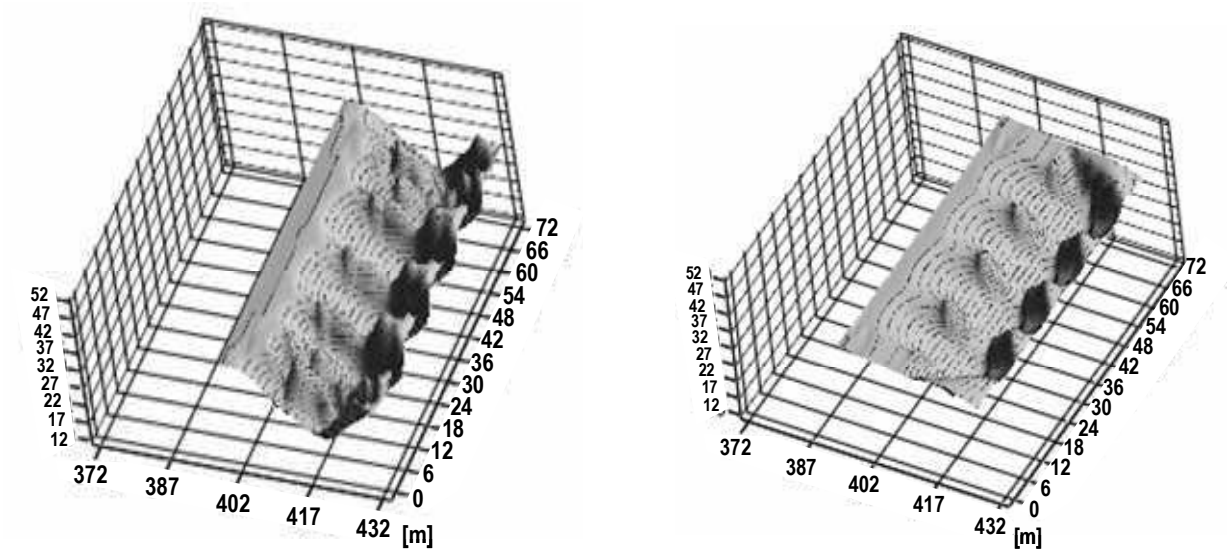

UPPER OUTLET WORKS LOWER OUTLET WORKS

Figure 6. 3D-shape of scour hole along the sloping part of the stilling basin bottom following a discharge of 3,300 cms and due to upper or lower pressurized outlet works functioning during 200 days (ultimate depth).

B. Emergency spillway flow scour formation

Potential scour formation downstream of the three emergency spillways has been determined for an extreme flood event of 8,500 cms (through these three gates only). Each emergency spillway gate has dimensions of 12 m by 15 m and generates a high-velocity free surface flow along a chute that ends with a flip bucket (Figures 1a & 2).

The flow from the flip bucket generates a rectangular shaped jet with a thickness of 8 m and a width of 15 m. The jet velocity at the flip is about 24 m/s. The jets are assumed to remain rectangular shaped during their fall and impact onto the downstream slab.

This slab is situated about 25-30 m higher than the stilling basin bottom and consists of a 1m thick concrete lining placed on dredge tailings of granular material between the left-sidewall of the stilling basin and the rock mass as shown in Figure 2. The tailings have a triangular cross-sectional shape that stays more or less constant in the longitudinal (flow) direction. The downstream part of the concrete lining of the slab has been partially damaged during past operation of the emergency spillways and has been repaired by placing a 3 m thick layer of lean concrete onto the dredge tailings, with a new reinforced concrete slab above that repair.

As the emergency jets might partially impact upstream of the repaired zone, and the concrete might fail or be uplifted more easily than the surrounding rock, this local reinforcement has not been accounted for in the present computations.

The results of the scour computations are summarized at Table 2 for that part of the slab that is located directly next to the stilling basin sidewall. Based on the Comprehensive Fracture Mechanics Model (CFM), scour formation only occurs after very long periods of extreme flooding (100 days or more) and consists of a very local destruction of the rock mass over a length of about 15-20 m. Nevertheless, for such periods of discharge, the

ultimate scour depth extends about 10 m beyond the elevation of the concrete slabs of the stilling basin. Its three-dimensional shape is presented in Figure 7. The scour hole has a length of about 15-20 m and a lateral width of 15 m.

The Dynamic Impulsion Model (DI) predicts much deeper scour than the Fracture Mechanics model, but this method uses the hypothesis that the rock mass consists of fully broken up rock blocks. This assumption is probably not plausible at large depths and not fully representative for the state of the rock mass.

Similar results for that part of the slab that is located further away from the sidewall of the stilling basin, at distances of more than 30 m, are summarized at Table 3. It can be noticed that the Fracture Mechanics approach indicates almost no scour formation, while the Dynamic Impulsion approach again results in significant scour formation. The same remark as for the first part of the plateau is valid here.

TABLE II. SCOUR RESULTS AT PLATEAU BENEATH EMERGENCY SPILLWAYS AND CLOSE TO THE STILLING BASIN SIDEWALL

		Ultimate Scour Elevation	Depth of Scour
	Flood duration	m a.s.l.	m
	h		
Fracture Mechanics Model	24 192 4800	no scour (50-55) 46 24.5	0 4-9 26-31
Dynamic Impulsion Model	infinity	17	33-38

TABLE III. SCOUR RESULTS AT PLATEAU BENEATH EMERGENCY SPILLWAYS AT 30 M DISTANCE FROM THE STILLING BASIN SIDEWALL

		Ultimate Scour Elevation	Depth of Scour
	Flood duration	m a.s.l.	m
	h		
Fracture Mechanics Model	24 192 4800	no scour (64) 64 61.5	0 0 2.5
Dynamic Impulsion Model	infinity	22.5	41.5

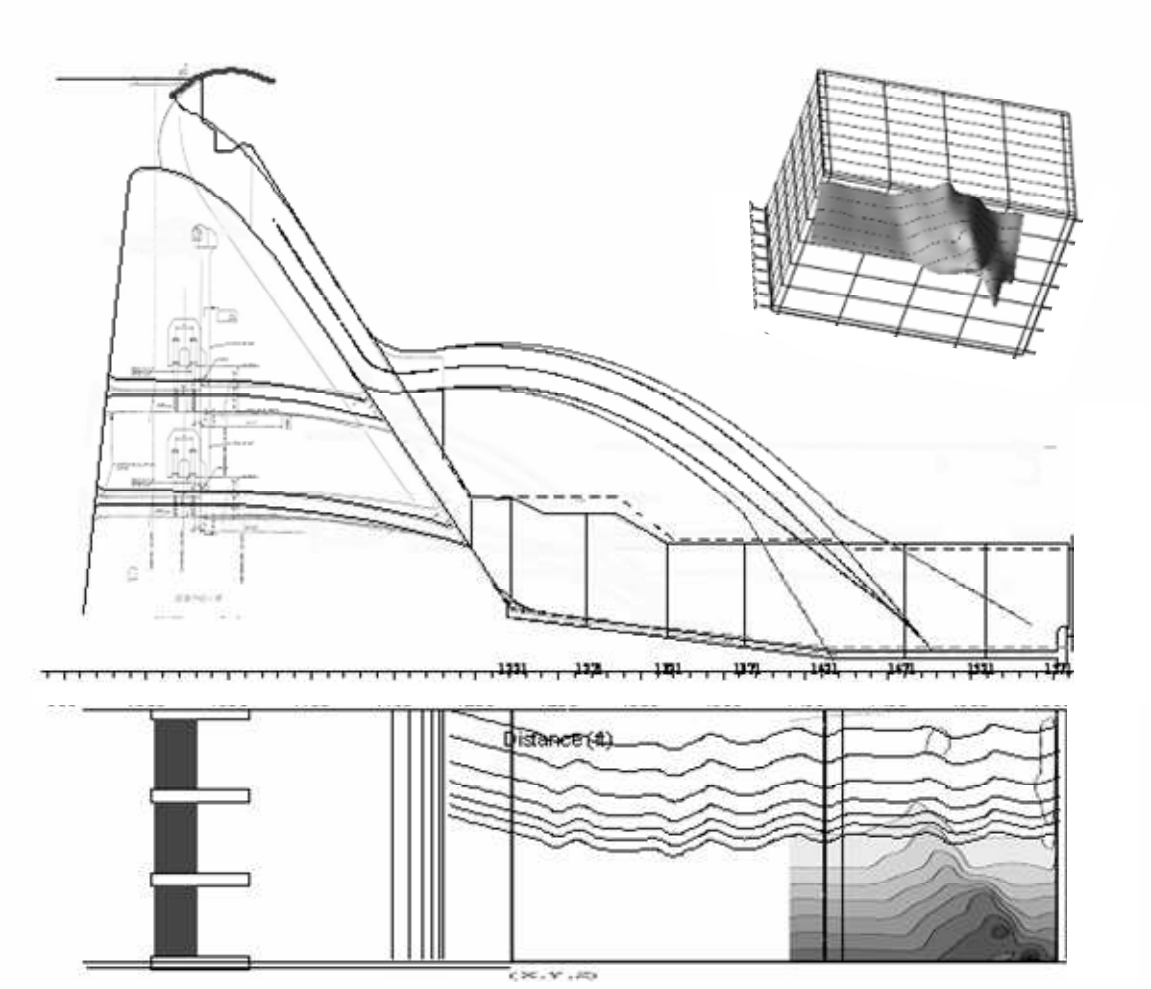

Figure 7. Emergency spillway scour: jet trajectory, zone of impact on the downstream concrete plateau and ultimate scour elevation for the parametric assumptions presented at Table 1.

VI. CONCLUSIONS

This Paper presents a new and physics based scour prediction model applicable to high-head hydraulic structures. The basics of the model are briefly outlined. The model has been applied to a High-Head Dam and Stilling Basin located in the United States.

The scour computations are based on the assumption that, during the flood event, one or more concrete slabs of the stilling basin fail. Scour is then computed in the underlying rocky foundation. The results of the scour computations indicate that, for a normal flood discharge of 3,300 cms, passing through the upper and lower tiers of the outlet works, only minor scour forms along the sloped (upstream) part of the stilling basin bottom. This scour forms almost completely within the first few days of the event. Subsequent scour formation takes much more time to happen. No danger for dam stability is apparent.

Second, scour formation following an operation of the three emergency spillway gates has been computed for a total discharge through these gates of 8,500 cms. The computations based on Fracture Mechanics result in scour depths of about 26-31 m after very long times of discharge (hundreds of days). This scour only forms locally, directly next to the left sidewall of the stilling basin, but may extend deeper than the concrete slabs of the stilling basin. Application of the Dynamic Impulsion Model indicates a scour hole of about 40 m deep. This model, however, assumes fully broken up rock at all depths and thus is too conservative.

Hence, it may be stated that, for an emergency flood through the emergency spillway gates, no significant scour will form into the downstream concrete plateau during the lifetime of the dam. Nevertheless, local minor scour may form and generate damage to the plateau.

REFERENCES

[1] Atkinson, B.K. (1987). Fracture Mechanics of Rock. Academic Press Inc., London.

[2] Bollaert, E.F.R. (2002). Transient water pressures in joints and formation of scour due to high-velocity jet impact. Communication 13, Laboratory of Hydraulic Constructions, Lausanne, Switzerland.

[3] Bollaert, E.F.R. (2004). A comprehensive model to evaluate scour formation in plunge pools. Int. J. Hydropower & Dams, 2004, 2004(1), pp. 94-101.

[4] Bollaert, E.F.R. and Schleiss, A.J. (2005), A physically-based model for evaluation of rock scour due to high-velocity jet impact, Journal of Hydraulic Engineering, March 2005.